Hybrid molecular-continuum simulations using smoothed dissipative particle dynamics

Nikolai D. Petsev, L. Gary Leal, and M. Scott Shell
Department of Chemical Engineering, University of California at Santa Barbara, Santa Barbara, California 93106-5080, USA

(Received 23 September 2014; accepted 26 December 2014; published online 22 January 2015)

We present a new multiscale simulation methodology for coupling a region with atomistic detail simulated via molecular dynamics (MD) to a numerical solution of the fluctuating Navier-Stokes equations obtained from smoothed dissipative particle dynamics (SDPD). In this approach, chemical potential gradients emerge due to differences in resolution within the total system and are reduced by introducing a pairwise thermodynamic force inside the buffer region between the two domains where particles change from MD to SDPD types. When combined with a multi-resolution SDPD approach, such as the one proposed by Kulkarni *et al.* [J. Chem. Phys. **138**, 234105 (2013)], this method makes it possible to systematically couple atomistic models to *arbitrarily* coarse continuum domains modeled as SDPD fluids with varying resolution. We test this technique by showing that it correctly reproduces thermodynamic properties across the entire simulation domain for a simple Lennard-Jones fluid. Furthermore, we demonstrate that this approach is also suitable for non-equilibrium problems by applying it to simulations of the start up of shear flow. The robustness of the method is illustrated with two different flow scenarios in which shear forces act in directions parallel and perpendicular to the interface separating the continuum and atomistic domains. In both cases, we obtain the correct transient velocity profile. We also perform a triple-scale shear flow simulation where we include two SDPD regions with different resolutions in addition to a MD domain, illustrating the feasibility of a three-scale coupling. © *2015 AIP Publishing LLC.* [http://dx.doi.org/10.1063/1.4905720]

I. INTRODUCTION

Numerous problems in molecular physics are characterized by multiple time and length scales, a feature that poses significant challenges in applying traditional simulation techniques. For instance, a problem involving localized nano-scale processes or phenomena at a solid surface in contact with a liquid may require molecular-scale resolution (e.g., molecular dynamics) for the solid-liquid boundary, whereas the bulk fluid region away from the surface may not necessitate this kind of detail, and an atomistic treatment of the full system may be prohibitively expensive from a computational standpoint. In fact, the problem of multiple characteristic length scales is one that frequently arises in fluid flow problems involving interfaces, such as the contact line of a three-phase flow,[1] slip along hydrophobic substrates,[2] and the dynamics of thin films.[3] Similarly, a broad range of problems involving biological molecules in explicit solvent (e.g., proteins) may not require the same level of detail for the solvent in the bulk far away from the molecule as in the region immediately surrounding it. In these cases, it is desirable to preserve a detailed description for the system in localized regions where necessary and use a simpler coarse-grained model, such as a continuum or mean-field approximation, for parts of the problem domain where less resolution is required.[4–8]

In light of this, there have been numerous efforts[1,9–15] to directly couple continuum-based (i.e., Navier-Stokes) solutions with molecular dynamics (MD). These studies have generally employed finite-difference/element/volume methods for the continuum region and transferred information between the continuum and MD domains via flux exchange within an overlap region. This is achieved by constraining the MD particle dynamics inside this region such that the averaged particle mass and momentum fluxes equal those in the overlapping continuum solution.[9,11] This approach was extended by Delgado-Buscalioni and De Fabritiis[12] by coupling MD to a finite-volume *fluctuating* continuum domain using the fluctuating hydrodynamic equations of Landau and Lifshitz.[16] However, flux exchange has been challenging in certain situations such as gas-phase calculations where fluctuations in the atomistic region can induce error and instability in the continuum solution.[17]

Alternatively, molecularly resolved and continuum domains may be coupled through the Schwarz alternating method, where state-exchange is achieved by matching boundary conditions and the individual regions are iterated until they converge to a steady-state solution.[1,10,18] Due to noise in the MD part of the system, fitting of the local velocity is necessary to smooth the boundary condition from the MD fluid that is applied to the continuum region in a given iteration. The Schwarz alternating method has already been used for multiscale simulations bridging the nano- and meso-scales in coupling MD and lattice Boltzmann domains.[19] Fedosov and Karniadakis[18] also adapted it to interface MD to a mesoscale region simulated using dissipative particle dynamics (DPD), which in turn was coupled to a numerical Navier-Stokes

solution. While this strategy decouples both time and length scales, it is less suitable for dynamic problems since each time-step is treated as quasi-steady-state and requires iteration, although often a single iteration per time-step may be sufficient for non-equilibrium systems.[1]

A different multiscale approach involves molecular to coarse-grained molecular coupling rather than molecular-continuum coupling, and one such strategy for interfacing atomistic models to a coarse-grained particle-based description has been proposed by Praprotnik *et al.*[20] The coarse-grained representation in their work is obtained from the molecular one by structure matching. Their "adaptive resolution scheme" (AdResS) then smoothly interpolates from the molecular to the coarse-grained particles as they pass between an atomistic region and a coarse-grained one.[20–26] Of course, a molecule's degrees of freedom are not conserved and continuously change as it traverses the intermediate region between the atomistic and coarse domains.[20] This method has been used to develop simulations of liquids with tetrahedral structure, including water, which are coupled to coarse-grained molecules with isotropic pair potentials obtained through Boltzmann inversion.[20,21,23,25,26] While it was originally described in the constant temperature case, recently this technique has been adapted for constant energy simulations, although the latter formulation results in a drift force such that momentum is only weakly conserved.[27] Importantly, this method has also been used in triple-scale simulations of water in which atomistic and coarse-grained mesoscale regions are coupled to a finite-volume continuum solution by exchange of fluxes between the different domains.[24] One issue of concern in such approaches is the lack of transferability in the coarse-grained model. Typically, the structure-matched coarse-grained potential is a function of the system thermodynamic state and thus simulating systems with temperature or density gradients, or across a variety of conditions, can be difficult to implement in a thermodynamically consistent manner.

Smoothed particle methods offer an alternative and particularly convenient approach to incorporating coarse-grained mesoscale and continuum regions in multiscale simulations, and this is the main strategy that we consider here. Particle-based continuum solvers include smoothed particle hydrodynamics (SPH)[28–30] and smoothed dissipative particle dynamics (SDPD).[31] In SPH, the problem domain is discretized into a set of Lagrangian particles or nodes. At each time step, the strain or strain-rate at a selected particle is computed from the particle velocities/positions in the system at that time. With the strain/strain-rate known, the stress at each particle is calculated from which the corresponding particle acceleration can be determined. Particle positions and velocities are integrated in time as in traditional MD,[30] although the equations of motion are distinct and formulated from a top-down, continuum assumption. Thus, SPH is essentially a method for numerically solving the hydrodynamic equations with a formalism that is reminiscent of MD.[30] SDPD is an extension of SPH to the mesoscale proposed by Español and Revenga that introduces thermal fluctuations in the field variables of the continuum solution.[31] In SDPD, the size of the fluid particles is determined by the choice of a parameter called the "smoothing length." Decreasing the smoothing length results in finer resolution and less massive particles that are subject to larger thermal fluctuations, whereas in the limit of large smoothing lengths, fluctuations disappear and continuum hydrodynamics in the form of SPH is recovered.

Particle-based solvers of the continuum equations offer a natural method of coupling with inherently particle-based descriptions of the molecular world. The use of discrete particle methods for all length scales in a multiscale simulation seems to have been first suggested by Dzwinel *et al.*[32] This perspective was subsequently adopted by Liu and Liu, who demonstrated that SPH can be stably coupled to MD.[30] These authors provide two possible schemes: (i) in the first approach, particles within an overlap region interact through both MD and SPH forces. (ii) In the second, force-bridging eliminates the need for an intermediate domain; MD particles interact through an atomic potential (e.g., Lennard-Jones), SPH particles interact through SPH forces, and at the interface between the two regions, MD and SPH particles interact symmetrically through some arbitrarily chosen interaction (SPH or MD). A similar approach was suggested by Ganzenmüller *et al.*,[33] who instead used an algebraic mean of MD and SPH forces for cross interactions. These techniques require a thermostat for the MD region since the (non-fluctuating) SPH particles otherwise dissipate all heat in the MD portion of the system through viscous interactions.

However, such coupling methods are not ideal if the smoothed particles are subject to fluctuations. For very small particles, the presence of thermal noise can lead a softly repulsive SPH particle to jump across an interface and instantaneously change type to a MD atom; since MD potentials frequently feature a steeply repulsive core, catastrophic forces result when such a particle enters the overlap region [approach (i)] or the MD region [approach (ii)] and lands close to another MD atom. Alternatively, if fluid particles are much larger than MD atoms such that fluctuations no longer yield large particle displacements per time-step, mass conservation requires performing particle insertions and deletions when particles cross the fixed boundaries. This is difficult to realize in an efficient manner that does not artificially disrupt either domain's equations of motion.

The tunability of the characteristic length scale (the smoothing length) makes SDPD an ideal candidate for multiscale simulation. Kulkarni *et al.*[34] demonstrated that it is possible to couple two SDPD regions with different resolutions (i.e., smoothing lengths) and reproduce correct thermodynamic equilibrium properties across an entire simulation box containing both domains. This opens the possibility for multiscale simulations spanning length scales from the mesoscopic to the continuum. Moreover, these authors showed that there is a smoothing length at the atomistic scale at which a collection of SDPD particles can successfully reproduce both dynamic and thermodynamic properties associated with a Lennard-Jones fluid. Therefore, coupling MD to a reduced-scale SDPD fluid seems to be the major missing link in using such methods to cover the spectrum of length scales from macroscopic to atomistic.

In this paper, we develop a technique for coupling an atomistic MD region to a fluctuating continuum solution obtained

using SDPD, which in turn can be coupled to increasingly coarse SDPD regions via the strategy of Kulkarni *et al.*[34] Instantaneously changing particle types at a sharp interface can incur catastrophic forces; hence, we follow the adaptive resolution approach and introduce a switching function such that particles change type gradually across an "overlap" region. For the atomistic region, we choose a Lennard-Jones fluid and demonstrate that with the method described here, correct thermodynamic properties are reproduced within the entire system. In order to reduce chemical potential gradients present due to differences in resolution, we introduce a pairwise thermodynamic force that performs work on the particles in the buffer region between the atomistic and continuum fluids. A derivation and discussion of this force is provided in Sec. IV. Finally, in Secs. VI and VII, we show that our method for coupling MD and SDPD correctly captures hydrodynamics by performing dual- and triple-scale simulations of shear flow. In order to illustrate the robustness of this approach, we consider two different cases: one in which shear forces act in a direction parallel to the interface between the continuum and atomistic region and one in which they are perpendicular.

II. SMOOTHED DISSIPATIVE PARTICLE DYNAMICS

Because it is the key element of the multiscale approach described in this paper, we first provide a brief summary of smoothed dissipative particle dynamics. To date, SDPD has been used to simulate a variety of mesoscale hydrodynamic phenomena including simple polymers,[35,36] pinned DNA subjected to shear flow,[37] colloidal particles,[35] the flow of blood,[38] suspensions,[39] and viscoelastic flows.[40] In this method, the domain is composed of a collection of particles or fluid volumes that evolve in time according to equations of motion obtained from a discretization of the fluctuating Navier-Stokes equations based on interpolation theory. The Navier-Stokes equation in Lagrangian form is[41]

$$\rho\frac{d\mathbf{v}}{dt} = -\nabla p + \eta\nabla^2\mathbf{v} + \left(\zeta + \frac{\eta}{3}\right)\nabla\nabla\cdot\mathbf{v}. \tag{1}$$

In applying the aforementioned particle discretization to this expression, it is possible to obtain an equation of motion for all the particles in the system, i.e., Eq. (1) can be solved numerically by deriving an appropriate interaction between particle pairs and integrating particle positions in time. The *reversible* contribution to the dynamics of particle i in the resulting equation is[31,35]

$$m_i\frac{d\mathbf{v}_i}{dt}\bigg|_{rev} = -\sum_{j=1}^{N} m_i m_j\left(\frac{p_i}{\rho_i^2} + \frac{p_j}{\rho_j^2}\right)\frac{\partial W_{ij}}{\partial r_{ij}}\mathbf{e}_{ij}, \tag{2}$$

where N is the number of particles in the system, p_i is the pressure at particle i, ρ_i is the density at particle i, m_i is the mass of the ith particle, W_{ij} is the smoothing kernel (discussed below), and $\mathbf{e}_{ij}$ is a unit vector joining the centers of particles i and j, $\mathbf{e}_{ij} \equiv \mathbf{r}_{ij}/|\mathbf{r}_{ij}|$ with $\mathbf{r}_{ij} \equiv \mathbf{r}_i - \mathbf{r}_j$. Equation (2) determines the force on particle i due to the local pressure distribution and corresponds to the discretization of the pressure gradient term in Eq. (1). The *irreversible*, viscous contribution to the Navier-Stokes dynamics is represented in SDPD by

$$m_i\frac{d\mathbf{v}_i}{dt}\bigg|_{irr} = \left(\frac{5\eta}{3} - \zeta\right)\sum_{j=1}^{N}\frac{m_i m_j}{\rho_i\rho_j}\left(\frac{1}{|\mathbf{r}_{ij}|}\frac{\partial W_{ij}}{\partial r_{ij}}\right)\mathbf{v}_{ij} + 5\left(\frac{\eta}{3} + \zeta\right)\sum_{j=1}^{N}\frac{m_i m_j}{\rho_i\rho_j}\left(\frac{1}{|\mathbf{r}_{ij}|}\frac{\partial W_{ij}}{\partial r_{ij}}\right)(\mathbf{v}_{ij}\cdot\mathbf{e}_{ij})\mathbf{e}_{ij}. \tag{3}$$

Here, η is the fluid shear viscosity, ζ is the bulk viscosity, and $\mathbf{v}_{ij} \equiv \mathbf{v}_i - \mathbf{v}_j$ is the relative velocity between particles i and j. The contribution of Eq. (3) to the SDPD equations of motion accounts for dissipative interactions between neighboring SDPD particles [i.e., the second and third terms on the right-hand side of Eq. (1)].

The last component of SDPD is the presence of thermal noise in the velocity field. Fluctuations are introduced in a thermodynamically consistent manner through the GENERIC[42–44] formalism and are described by[31,45]

$$m_i d\tilde{\mathbf{v}}_i = \sum_{j=1}^{N}\left(A_{ij}d\hat{\mathbf{W}}_{ij} + \frac{1}{3}B_{ij}\mathrm{tr}[d\mathbf{W}_{ij}]\mathbf{I}\right)\cdot\mathbf{e}_{ij} \tag{4}$$

$d\mathbf{W}_{ij}$ is a tensorial generalization of the stochastic Wiener process,[68] and $d\hat{\mathbf{W}}_{ij}$ is the traceless, symmetric part of $d\mathbf{W}_{ij}$, i.e., $d\hat{W}_{ij}^{\alpha\beta} = \frac{1}{2}\left[dW_{ij}^{\alpha\beta} + dW_{ij}^{\beta\alpha}\right] - \frac{\delta^{\alpha\beta}}{3}\mathrm{tr}[d\mathbf{W}_{ij}]$. The form of this random contribution to the dynamics is postulated such that it is consistent with the tensorial structure of the friction forces in the hydrodynamic equations.[45] This final contribution to the equations of motion is the force on particle i due to random stresses induced by thermal fluctuations in the fluid. Fluctuation-dissipation is satisfied by the following choice for the magnitudes of the noises A_{ij} and B_{ij}:

$$A_{ij} = \left[-\frac{4m_i m_j k_B T}{\rho_i\rho_j}\left(\frac{5\eta}{3} - \zeta\right)\left(\frac{1}{|\mathbf{r}_{ij}|}\frac{\partial W_{ij}}{\partial r_{ij}}\right)\right]^{1/2},$$
$$B_{ij} = \left[-\frac{4m_i m_j k_B T}{\rho_i\rho_j}\left(\frac{5\eta}{3} + 8\zeta\right)\left(\frac{1}{|\mathbf{r}_{ij}|}\frac{\partial W_{ij}}{\partial r_{ij}}\right)\right]^{1/2}. \tag{5}$$

Equations (2)–(4), together with the noise magnitudes given in Eq. (5), collectively yield a set of stochastic differential equations governing the velocity field for a SDPD fluid at constant temperature. All these terms, including the viscous and random forces, act symmetrically on pairs of particles so that momentum is conserved; in other words, particle forces are pairwise and depend only on the position and velocity difference vectors.

The smoothing kernel W_{ij} is an even, monotonically decreasing function of the particle separation r_{ij} with compact support, normalized to unity. Here, we use the cubic spline,[30,34,46,47]

$$W_{ij}(q) = \frac{1}{\pi h^3}\begin{cases} 1 - \frac{3}{2}q^2 + \frac{3}{4}q^3, & 0 \le q < 1, \\ \frac{1}{4}(2-q)^3, & 1 \le q < 2, \\ 0, & q \geqslant 2, \end{cases} \tag{6}$$

where $q = r_{ij}/h$. The support domain of a point is determined by the smoothing kernel and equals κh, where $\kappa = 2$ for the cubic spline. While the sums in Eqs. (2)–(4) extend over all the particles in the system, the compact support condition

for the weighting function implies that only nearby particles contribute to the sums.

In the SPH and SDPD approximations, field variables and their spatial derivatives are calculated from a weighted average using properties associated with nearby particles, where the weight is determined by the kernel W_{ij} or its derivative, respectively, at the neighboring particle's location. For instance, the density at particle i is simply a weighted average over neighboring particle masses,

$$\rho(\mathbf{r}_i) = \sum_{j=1}^{N} m_j W(\mathbf{r}_i - \mathbf{r}_j, h). \tag{7}$$

The density field is updated at each time-step by performing this sum; an alternative approach is to use a discretized form of the continuity equation.[30] Note that a different density is obtained from Eq. (7) depending on whether particle i itself contributes to the sum. Generally, the particle's own contribution should be included since the particle distribution for a SPH fluid has order,[48] although for small smoothing lengths where the distribution of particles is more disordered due to thermal noise, this can lead to an overestimated density.[34,48,49] In the present work, we include the self-contribution to density. This is an important subtlety that is revisited in Secs. IV and V.

Solid boundaries in a SDPD region are treated as a collection of SDPD particles frozen on a lattice; for a wall-fluid particle pair interaction, a velocity is calculated and assigned to the wall particle such that no-slip is enforced at the boundary. The details of this approach are described in Ref. 50, as well as in the supplementary material.[51] Due to the high diffusivity of SDPD particles with a very small smoothing length, additional measures such as specular reflection, a higher wall particle number density, additional interparticle forces,[30] or velocity averaging[30,31,52] may be necessary to fully prevent boundary penetration.

III. ADAPTIVE RESOLUTION SCHEME FOR COUPLING MD TO SDPD

We couple MD to SDPD using the adaptive resolution scheme (AdResS) proposed by Praprotnik *et al.*[20] This makes it possible to define a fixed overlap domain between the two regions where particles continuously change type from MD to SDPD and vice versa. In this scheme, *reversible* particle pair interactions are turned on/off via a weighting function that depends on their positions within the transition domain. Particles within the MD region interact through an atomistic potential and in the SDPD domain, particles interact through SDPD forces [Eqs. (2)–(4)]. Within the overlap region, particles interact through a linear combination of both interactions, as described below. AdResS has been considered in the context of coupled MD/finite-volume continuum solutions previously,[24] but has not been used with particle-based continuum solvers (e.g., SDPD), even though they present a natural option since one only has to consider particle-particle interactions. Importantly, through this kind of pairwise MD-SDPD coupling, thermal noise in the MD region will not lead to error in the continuum solution since fluctuations are already present in SDPD. Moreover, one can avoid particle insertions and deletions by scaling down the smoothing length of the SDPD fluid such that the SDPD particles are identically massive to the MD particles. This SDPD domain with atomistic resolution can then be coupled to more coarse SDPD regions using the method of Kulkarni *et al.*[34] An attractive feature of the AdResS approach is that it can be used for coupling to atomistic fluids with complicated molecular geometries.[20–23,25,26]

To implement AdResS, we define a switching function $s(z)$ that is zero in the SDPD domain, unity in the MD domain, and smoothly and monotonically transitions between these two values in the buffer region. An example of such a function is shown in Fig. 1. With this switching function, it is possible to define the quantity $\lambda = s(z_i)s(z_j)$, which can be used (as shown below) to interpolate between pairwise particle forces and continuously change particle types within the buffer region. Hence, reversible interactions between particle pairs can be written as a linear combination between the atomistic MD forces and reversible SDPD forces [Eq. (2)],[20]

$$\mathbf{F}_{ij}\big|_{rev} = \lambda \mathbf{F}_{ij}^{MD} + (1-\lambda)\mathbf{F}_{ij}^{SDPD}\big|_{rev}. \tag{8}$$

The form for the MD force depends on the interatomic potential. More generally, Eq. (8) describes the reversible dynamics across the entire simulation domain; for example, for particle pairs in the MD region, $s(z)$ for both particles is equal to unity, and thus the second term vanishes, leaving only MD interactions, as we would expect. Similarly, if both particles are within the SDPD region, λ is zero for the pair and the first term involving MD forces vanishes, and the reversible dynamics are described by Eq. (2). Note that for the buffer region ($0 < \lambda < 1$), the weighting by λ is only applied to the reversible part of the dynamics, and the viscous and random forces [Eqs. (3) and (4)] are applied to *all* buffer particles without weighting. This is done in order to thermostat the buffer to the correct temperature and is discussed in more detail below. Because Eq. (8) interpolates between pairwise forces, momentum is conserved.

For a simple two-scale AdResS system with periodic boundary conditions in all directions and a vector normal to the two overlap or "buffer" regions between the MD and SDPD regions in the z-direction (Fig. 1), an example for the aforementioned weighting function used for interpolating forces inside a buffer bounded by $z = z_{min}$ and $z = z_{max}$ is[20]

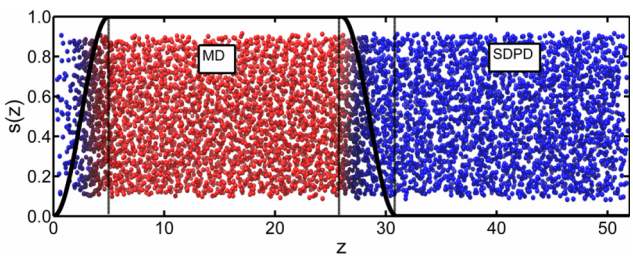

FIG. 1. Adaptive resolution weighting function versus position in the problem domain (dark black curve). A snapshot of the system is superimposed for clarity. The part of the domain where $s(z) = 1$ is the MD region, the part where it is zero is the SDPD region, and particles within the remaining "buffer" domains interact through a linear combination of both MD and SDPD forces.

$$s(z) = \sin^2\left[\frac{\pi}{2}\left(\frac{z - z_{min}}{z_{max} - z_{min}}\right)\right], z_{min} \le z \le z_{max}. \quad (9)$$

This function smoothly transitions from a value of zero in the SDPD domain to unity in the MD region. A similar function may be defined for the second buffer, which is necessary due to the simulation domain periodicity. The form for the global switching function is shown in Fig. 1, together with a superimposed example snapshot of the simulation box for a simple system with periodic boundary conditions in all directions.

Additional care is necessary to address the manner in which the MD potential is switched on/off within the buffer since it typically contains a steeply repulsive core. In this work, we choose a Lennard-Jones (LJ) potential for the MD region, which diverges at zero particle separation. The sudden onset of LJ interparticle forces at the MD/buffer interface when λ becomes nonzero can be catastrophic if the SDPD particle enters the buffer region close to another particle. Praprotnik *et al.* remedy this issue by capping the atomistic interactions.[20] Instead of this approach, we use the weight parameter λ to gradually switch on the atomistic repulsive forces. Specifically, within the buffer region we use core-softened LJ interactions[53] that continuously approach the normal LJ interactions with decreasing distance from the LJ/buffer interface,

$$\mathbf{F}_{ij}^{MD}(r_{ij}, z_i, z_j) = \begin{cases} 24\varepsilon_{ij} r_{ij}^5 \left(\dfrac{2\sigma_{ij}^{12}}{\left[(1-\lambda)\sigma_{ij}^6 + r_{ij}^6\right]^3} - \dfrac{\sigma_{ij}^6}{\left[(1-\lambda)\sigma_{ij}^6 + r_{ij}^6\right]^2} \right) \mathbf{e}_{ij} & , r_{ij} \le r_c, \\ \mathbf{0} & , r_{ij} > r_c. \end{cases} \quad (10)$$

Here, σ_{ij} and ε_{ij} set the length scale and energy for the interaction, respectively, and r_c is the cut-off radius. For the case of $\lambda = 1$, this expression reduces to the familiar LJ force. Even with these measures, an insufficiently small time-step may still lead to instability, although we find that this scheme is stable for typical MD simulation time-steps. It is worthwhile to note that the core-softened LJ potential is frequently used in alchemical free energy calculations that introduce and remove atoms and their interactions for related numerical reasons.[54]

Finally, it is necessary to apply a thermostat either to the full system or to the buffer region when using the AdResS approach.[20,21] The two domains in such a dual-scale simulation can be considered as different phases in equilibrium,[20,21,26] with a corresponding latent heat for particles traveling between the atomistic and coarse regions. Without a thermostat, the loss of heat that occurs within the buffer region results in a MD domain at a lower temperature than the SDPD region that is by construction thermalized to the correct temperature. This undesirable temperature imbalance leads to a pressure differential that is relaxed by a transfer of mass into the MD region, resulting in a non-uniform density distribution. This issue is resolved by applying a thermostat to the entire buffer region. In this study, we use the SDPD thermostat, i.e., the irreversible and stochastic SDPD forces [Eqs. (3) and (4)] act on all buffer particles without any weighting by the parameter λ, and the switching function is only used to interpolate between the MD and SDPD reversible dynamics. Hence, at one end of the buffer, the particles are simply a SDPD fluid, while at the other end they are a MD fluid coupled to a SDPD thermostat. This thermostat is similar to the DPD thermostat[55,56] that is frequently used in molecular dynamics simulations, which also introduces pairwise viscous and random forces between particles. The pure MD region itself is not thermostatted but is still held at fixed temperature due to its interface with the buffer, and thus the correct deterministic dynamics in the MD region are preserved. We note that in addition to AdResS, hybrid explicit/implicit solvent approaches also typically require a similar stochastic buffer region,[4,5] as do multiscale simulations using flux exchange[9] and the Schwarz alternating method.[10]

IV. PAIRWISE THERMODYNAMIC FORCE

The unphysical mixture of interparticle forces within the buffer region [Eq. (8) and Fig. 2] can lead to deviations from the target density at equilibrium. For example,

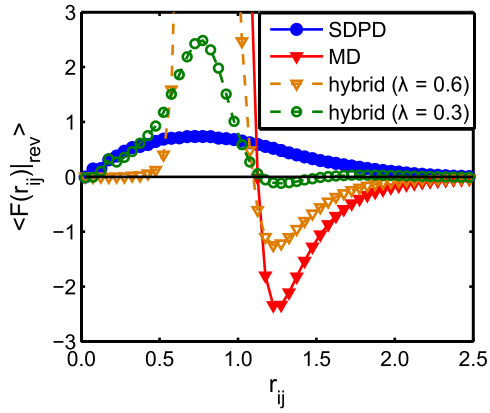

FIG. 2. Effective time-averaged force-versus-separation between particle pairs as a function of position within the buffer. Curves were obtained from simulations where all the particles in the system interact through either pure MD or SDPD forces, or some linear combination of the two that is constant throughout the simulation domain. The red (solid triangle) and blue (solid circle) curves denote the force between pure MD and SDPD particles, respectively. The green (hollow circle) and orange (hollow triangle) curves indicate the hybrid force at two different points within the buffer region. The results show that hybrid particles with λ between 0 and 1 can experience effective repulsions corresponding to a modified particle size.

Lennard-Jones particles experience both attractions and stiff repulsions, whereas SDPD particles are subject to an effectively soft-repulsive many-body force. A mixture of these two fundamentally different forces can result in particles with very different properties (e.g., effective size, attraction, and repulsion) than either of the two original interactions alone—for instance, mixed particles may have a repulsive core at a smaller radius, which leads to a local density increase at equilibrium. Similarly, the mixture of these forces could lead to a larger effective particle size and yield a region of depleted density. The specific implementation of λ in the selected MD potential [e.g., Eq. (10)] also affects how the effective particle diameter changes with position within the buffer. The emergence of a non-uniform equilibrium density distribution in the transition region can be viewed in terms of chemical potential gradients due to mixed particles. Indeed, simulations using the hybrid methodology described above show significant deviations from the target density in the buffer if no means are taken to correct this [red curve, square markers, Fig. 3(b)].

To compensate for these unphysical deviations from the target density, we can introduce a "thermodynamic" force that performs work on the particles within the transition region such that the density remains approximately flat. A loose physical interpretation of this work is that it gives the necessary effort required to remove or add degrees of freedom to a particle as it transitions from one type to the other. A similar approach has already been rationalized and tested in work using AdResS;[25,26] specifically, Fritsch *et al.* introduced a thermodynamic force of the form[26]

$$\mathbf{F}^{th} = \frac{m}{\rho_0}\nabla p(\mathbf{r}). \tag{11}$$

To a linear approximation, the force acting on particle i can be rewritten as

$$\mathbf{F}_i^{th} = -\frac{m_i}{\rho_0^2 \kappa_T}\nabla \rho(\mathbf{r}_i), \tag{12}$$

where κ_T and ρ_0 denote the isothermal compressibility and density, respectively, of the fluid at the desired thermodynamic state. Here, the pre-factor $1/\rho_0^2\kappa_T$ is interpreted as the variation of the local chemical potential due to changes in density,[26] since $(\partial\mu/\partial\rho)_T = 1/\rho^2\kappa_T$. It is clear that Eq. (12) applies a force to particles only in the presence of density gradients and that the force promotes particles to move from regions of higher to lower densities, i.e., opposite the gradient.

In order to determine the form for the thermodynamic force, it is necessary to perform a reference simulation and obtain the density profile within the buffer through a binning procedure. With the density profile known, Eq. (12) can be used to numerically determine an optimal force as a function of position. Then, a new simulation can be performed using this force and the new density distribution will appear "flatter." Subsequent modifications to the force may need to be applied through iterations of Eq. (12) and additional test simulations until the density distribution is deemed sufficiently flat. A potential drawback of this type of force is that it is single-body and position-dependent, resulting in loss of momentum conservation within the simulation domain.

The ideas above can be reformulated in a particularly convenient way that also leads to improved behavior for the present scenario involving SDPD particles. For our problem, we have access to the instantaneous density distribution at every time-step since we calculate SDPD interactions within the buffer; therefore, we seek to write an equivalent thermodynamic force that acts in real-time and does not require iterative simulations. Moreover, we would like to symmetrize this correction force such that it is pairwise and momentum is conserved. First, we write the thermodynamic force as

$$\mathbf{F}_i^{th} = -\frac{m_i}{\rho_0^2 \kappa_T}\frac{1}{\rho(\mathbf{r}_i)}[\rho(\mathbf{r}_i)\nabla\rho(\mathbf{r}_i)]. \tag{13}$$

Since $\rho(\mathbf{r}_i)\nabla\rho(\mathbf{r}_i) = (1/2)\nabla\rho^2(\mathbf{r}_i)$, this expression may be rewritten as

$$\mathbf{F}_i^{th} = -\frac{m_i}{2\rho_0^2 \kappa_T}\frac{1}{\rho(\mathbf{r}_i)}\nabla\rho^2(\mathbf{r}_i) = -\frac{m_i}{2\rho_0^2 \kappa_T}\frac{1}{\rho(\mathbf{r}_i)}\nabla\left[\rho^2(\mathbf{r}_i) - \rho_0^2\right]. \tag{14}$$

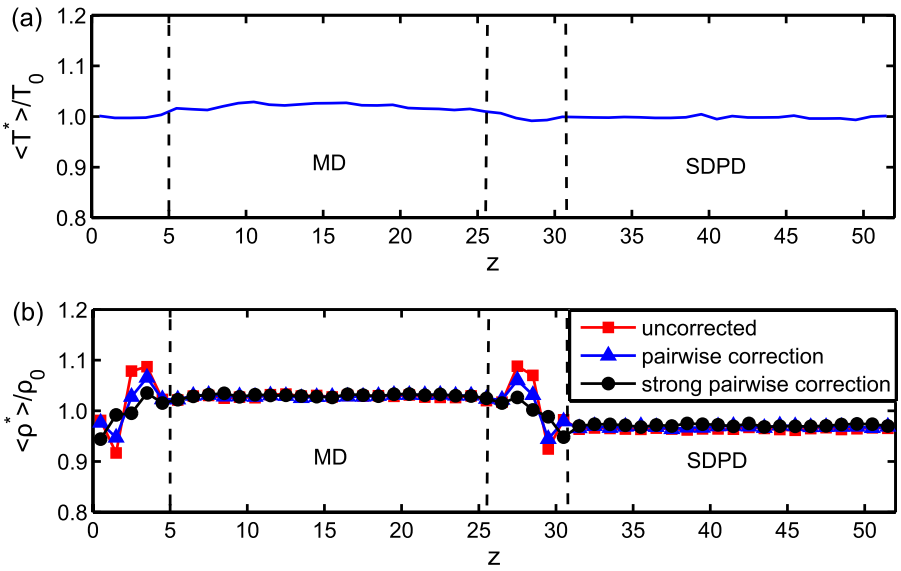

FIG. 3. (a) Temperature profile for a LJ system coupled to a SDPD domain at equilibrium with a pairwise correction force. The profile is approximately flat, with deviations less than 2.0% from the target temperature. (b) Density profiles for the system. The red curve (squares) is the density without corrections, while the blue curve (triangles) is with a pairwise correction. The densities within the MD/SDPD domains are within 3.2% of the target value with this correction. The black curve (circles) is the density profile when the strength of the pairwise thermodynamic force is increased by a factor of 10. For the MD and buffer regions, densities are computed by binning the system and counting particles, while for the SDPD part of the system, we use the SPH calculation for density [Eq. (7)] at randomly sampled points.

Let $g(\mathbf{r}_i) \equiv \rho^2(\mathbf{r}_i) - \rho_0^2$ and note that we can write

$$\mathbf{F}_i^{th} = -\frac{m_i}{2\rho_0^2\kappa_T}\left[\nabla\left(\frac{g_i}{\rho_i}\right) + \frac{g_i}{\rho_i^2}\nabla\rho_i\right]. \tag{15}$$

Here, we have used the shorthand $g_i \equiv g(\mathbf{r}_i)$. In the SPH approximation, the gradient operator can be expressed as a sum over particles such that

$$\begin{aligned}\mathbf{F}_i^{th} &\approx -\frac{m_i}{2\rho_0^2\kappa_T}\left[\sum_{j=1}^{N}\frac{m_j}{\rho_j}\frac{g_j}{\rho_j}\nabla_i W_{ij} + \frac{g_i}{\rho_i^2}\sum_{j=1}^{N}\frac{m_j}{\rho_j}\rho_j\nabla_i W_{ij}\right] \\ &= -\frac{m_i}{2\rho_0^2\kappa_T}\sum_{j=1}^{N} m_j\left(\frac{g_i}{\rho_i^2} + \frac{g_j}{\rho_j^2}\right)\nabla_i W_{ij}.\end{aligned} \tag{16}$$

Therefore, we arrive at a pairwise thermodynamic force

$$\frac{\mathbf{F}_i^{th}}{m_i} = -\frac{1}{2\rho_0^2 k_T}\sum_{j=1}^{N} m_j\left[\frac{\left(\rho_i^2-\rho_0^2\right)}{\rho_i^2} + \frac{\left(\rho_j^2-\rho_0^2\right)}{\rho_j^2}\right]\frac{\partial W_{ij}}{\partial r_{ij}}\mathbf{e}_{ij}. \tag{17}$$

In the SPH approximation, the subtracted constant ρ_0 should vanish due to the antisymmetry of the weighting function derivative for a completely uniform particle distribution. If the particles are not distributed uniformly, the subtracted constant will lead to a non-zero contribution to the pairwise correction force and hence penalize deviations from a flat distribution. Note that Eq. (17) is equivalent to the reversible SDPD force [Eq. (2)] if we choose the following equation of state:

$$p_i = \frac{1}{2\rho_0^2\kappa_T}\left(\rho_i^2 - \rho_0^2\right). \tag{18}$$

The equation of state for a system that is a linear combination of two systems with identical equations of state may not necessarily be the same as that in the two individual regions[21] and hence we can also think of this thermodynamic force as a modification to the SDPD equation of state within the buffer that minimizes density gradients. Note that both the iterative and SDPD thermodynamic forces are independent of the specific choice for the MD interaction potential and are thus quite general. Here, the density ρ_0 includes the particle self-contribution (discussed in Sec. II) since the force depends on the density defined at each particle, which will be overestimated for small smoothing lengths. Importantly, the force described by Eq. (17) is pairwise in form and thus conserves momentum. This pair force is zero if the density at both particles is precisely equal to the target density, as we would expect. If both particles occupy a high-density region and their densities are higher than the target value, the net force will be repulsive and drive them apart. If both particles are in a low-density region, the net force will be attractive and thus impede the particles from separating.

One final modification to the thermodynamic force ensures that it only applies to mixed particles in the buffer region and continuously vanishes as both particles approach either the pure MD or SDPD domains. This is achieved by using the switching function $s(z_i) \equiv s_i$ [Eq. (9)] to define a weighting parameter $\xi = 2[s_i(1-s_j) + s_j(1-s_i)]$ for the thermodynamic force, ensuring that it contributes maximally in the buffer center and vanishes at the boundaries. Hence, Eq. (8) is modified to include the pairwise thermodynamic force so that the reversible dynamics in the buffer are given by

$$\mathbf{F}_{ij}^{buffer}\Big|_{rev} = \lambda\mathbf{F}_{ij}^{MD} + (1-\lambda)\,\mathbf{F}_{ij}^{SDPD}\Big|_{rev} + \xi\mathbf{F}_{ij}^{th}. \tag{19}$$

V. TEST OF MD-SDPD COUPLING AT EQUILIBRIUM

In order to test this methodology, we first ensure that the coupling scheme yields proper thermodynamic equilibrium, that is, thermodynamic properties like the density and temperature remain uniform across the simulation domain containing both SDPD and MD regions. As a case study, we consider a simple Lennard-Jones fluid with periodic boundary conditions in all directions, as illustrated in Fig. 1. Values are reported in reduced Lennard-Jones units and all atoms have a mass of unity. The extent to which MD particles interact with their local environment is determined by the potential cut-off radius r_c, whereas the extent for the SDPD interaction depends on the particles' influence domain κh. Hence, we can ensure symmetric interactions and momentum conservation for the hybrid particles by equating the cut-off radius for the MD potential to the influence domain of the SDPD particles. The latter is chosen so that the SDPD particles are identically massive to the MD atoms ($h = 1.3$). Since $\kappa = 2$ for the cubic spline, it follows that $\kappa h = r_c = 2.6$. MD atoms are held at fixed temperature due to interactions with the buffer particles, which are thermalized using the SDPD thermostat as described in Sec. III. The simulation box features a SDPD domain adjacent to a MD domain with identical dimensions, where the two are separated by buffer regions using the AdResS approach described in Sec. III. Periodic boundary conditions are used in the x-, y-, and z-directions, and the z-direction is normal to the interface separating the MD and SDPD regions.

A snapshot of the simulation domain is provided for clarity in Fig. 1 together with the switching function appropriate to this problem geometry. The pure MD and SDPD regions of the simulation domain have dimensions $L_x = L_y = 13$ and $L_z = 21$ with a reduced density of $\rho = 0.79$. Particles are initialized on a square $12\times12\times48$ lattice inside of a box with dimensions $13\times13\times52$, with those between $z = 0$ and $z = 5$ (and $z = 26$ and $z = 31$) designated as buffer particles. Hence, there are a total of 6912 particles. The region between $z = 5$ and 26 is the MD domain and between $z = 31$ and 52 is the SDPD one. The MD and SDPD regions are separated by buffers of width 5. The target temperature is $T = 1.0$, and the fluid bulk and shear viscosities are $\zeta = 0.9$[57] and $\eta = 1.9$,[58,59] respectively. For time-integration, we use a modified velocity-Verlet algorithm where SDPD viscous forces are determined from an extrapolated velocity computed at the previous time-step,[55] and we choose a time-step of $\Delta t = 0.002$. The system is equilibrated for 2×10^5 time-steps, and data are averaged over 1×10^5 time-steps.

In pure SDPD simulations, the fluid thermodynamic properties are specified by the equation of state, which is used to obtain the pressure distribution that determines the reversible dynamics given by Eq. (2). For simulations of incompressible fluids, a common choice for the equation of state is $p_i = c_s^2\rho_i$,[30] where c_s is the speed of sound. The parameter c_s is often selected based on convenience such that small density variations yield large pressure gradients, yet

not so large that an impractically small time-step is required (i.e., such that the fluid is actually quasi-incompressible). However, the above equation of state cannot be used directly for MD/SDPD multiscale simulations since the speed of sound of a Lennard-Jones fluid in reduced units at this thermodynamic state is $c_s = 5$,[34] which would result in an excessively high pressure in the SDPD domain and drive a flux of mass into the MD region. Furthermore, for a SDPD fluid characterized by a small smoothing length, the density and hence pressure at a given particle is overestimated due to self-contribution effects (discussed in Sec. II). Therefore, we modify the aforementioned linear equation-of-state to ensure that the absolute pressure is not altered by changing the speed of sound,

$$p_i = c_s^2(\rho_i - \rho_0) + p_0. \tag{20}$$

Here, p_0 is the target pressure, and ρ_0 is the target density including the overestimation due to self-contribution to density. This expression is simply a local, linear approximation to the full equation of state where the absolute pressure and compressibility can be adjusted independently, hence making it possible to use the appropriate value for the speed of sound and thus match both compressibility and absolute pressure to the target fluid. For the temperature and density investigated here, the target pressure for the LJ fluid with a cut-off $r_c = 2.6$ is $p_0 \approx 1.4$. For SDPD particles with a smoothing length of $h = 1.3$, the overestimated averaged density at each particle from Eq. (7) is found to be $\rho_0 \approx 0.804$, which is slightly larger than the actual value of 0.787 due to self-contribution effects. This discrepancy is important to note: this overestimated SDPD density should be used as the target density in the above equation of state and the pairwise thermodynamic force since both of those quantities depend on the density defined at each particle. This quantity can be obtained by running an inexpensive pure SDPD simulation at the desired thermodynamic state and averaging particle densities. From equilibrium MD simulations, we find that the compressibility of a LJ fluid at the selected thermodynamic state is $\kappa_T \approx 0.08$, and hence the pre-factor for the thermodynamic force is $1/2\rho_0^2\kappa_T \sim 10$.

The overall approach just described is tested in the absence of flow fields. We find that thermal equilibrium is readily achieved and the pure MD and SDPD fluids converge within 2.0% accuracy to the correct temperature as estimated from the particle kinetic energies. Namely, there are no significant temperature gradients in the direction normal to the interface between the two domains [Fig. 3(a)]. This accuracy can be further improved by coupling the buffer more strongly to a thermostat or applying a thermostat to the full system. Moreover, the density profile in the system is approximately flat. Fig. 3(b) shows the density profile in the z-direction with and without the pairwise thermodynamic correction force. While the former exhibits some unphysical deviations in the buffer region from the target value, it is improved relative to the case without the thermodynamic force. The uncorrected density profile is within 2.8% and 3.6% of the target value within the MD and SDPD regions, respectively, with more substantial deviations in the buffer. With this force, the average densities inside the MD and SDPD regions are both within 2.9% and 3.2%, respectively, and the deviations inside the buffer are noticeably reduced. The flatness of the density distribution can also be further improved by increasing the prefactor in the pairwise corrective force. Increasing the strength of this force by a factor of 10 reduces deviations in the buffer further and lowers the error in the pure MD and SDPD region to less than 2.9%. Finite-size effects appear to have a measurable, albeit weak, influence on this approach. We have performed equilibrium tests in the absence of a thermodynamic force with bulk MD/SDPD regions twice as large as the case discussed above, as well as twice as small. Increasing the volume of the bulk MD and SDPD regions by a factor of four, while keeping the buffer domains identical in size, leads to a change in the density in the SDPD region from 0.756 to 0.760 and from 0.805 to 0.810 in the MD region.

We have also investigated fluctuations in key quantities for the equilibrium case. By construction, the multiscale method correctly captures fluctuations in velocity and reproduces the appropriate Maxwell-Boltzmann statistics throughout the entire simulation domain. The standard deviation of the density in the MD, SDPD, and buffer regions is $\sigma_\rho \approx 0.027$, 0.042, and 0.036, respectively. These results suggest that the compressibility is approximately matched in all three regions; a more careful choice for the speed of sound in the equation of state [Eq. (20)] may improve these results. We also note that the unphysical deviations from the target density will affect the compressibilities, and hence some non-uniformity between the compressibility values is expected. Finally, the soft potential in the coarse-grained SDPD domain leads to a slightly higher diffusivity than in the MD region, which is a common feature of coarse-grained systems, and hence mass diffusivity is not completely uniform across the full simulation domain.

We find that the density profile can be further flattened through several approaches. One alternative is to use the iterative non-pairwise thermodynamic force, Eq. (12). In principle, with a sufficient number of iterations and appropriate choice for a thermostat, it is possible to obtain a flat density profile to arbitrary precision using this force. This approach would be less suited for non-equilibrium problems, however, since it does not conserve momentum and may require strong thermostatting. Alternatively, since the Navier-Stokes solution does not depend on the absolute pressure of the fluid, we can adjust the p_0 parameter in the SDPD equation of state [Eq. (20)]. Reducing its value to $p_0 = 0.5$, we find that the error in density in the pure MD and SDPD regions is improved to 0.5% and 1.2%, respectively. It may be possible to reduce the error even further with a more careful tuning of p_0. Finally, the unphysical density deviations in the buffer region can also be reduced by implementing a three-part overlap domain. In this approach, the MD-to-SDPD and SDPD-to-MD transition regions are separate, with a MD/SDPD coexistence region between them where particles of different types interact via SDPD forces. This approach will be the subject of future work.

VI. NON-EQUILIBRIUM CASES INVOLVING THE START UP OF SHEAR FLOW

To levy a more challenging test, we ask how accurately the hybrid method reproduces the correct dynamical behavior in a

non-equilibrium scenario, when fluxes of momentum and mass must be preserved across the buffer region. We again consider a Lennard-Jones fluid but in a slab geometry confined between two solid interfaces. After equilibration, we subject it to the start up of shear flow by moving one of the solid boundaries with a constant velocity. In order to demonstrate the robustness of this multiscale technique, we consider two distinct cases: (1) shear forces act in a direction perpendicular to the interface separating the atomistic and continuum regions and (2) shear forces act in a direction parallel to the buffer region. In the former case, particles are actually convected by the shear forces through the buffer region and thus in some sense are forced (by the flow) to change type. In the latter, particles are not convected across the buffer region but diffuse on their own through Brownian motion. For all of the non-equilibrium simulations considered, we apply the pairwise correction force (Sec. IV) and SDPD thermostat (Sec. III) in the buffer so that momentum in the fluid is conserved.

In the perpendicular case, fluid is convected across the buffer region between the MD and SDPD domains due to the motion of the solid boundary, as illustrated in Fig. 4(a). Wall particles within the atomistic region are treated as Lennard-Jones atoms tethered to a fixed position in space using a harmonic potential with a force constant $k = 1000$. For the moving wall, the equilibrium positions of the harmonic potential for the boundary particles are translated at the appropriate velocity. When these atoms enter the buffer region, harmonic forces are turned off and the particles freeze at their instantaneous positions, at which point they are translated at the wall velocity. These transitional wall particles interact with LJ wall particles through pure LJ interactions and with fluid particles in the buffer through AdResS mixed forces, as described previously. We use an Andersen thermostat for the wall particles in the MD region. Cross interactions involving hybrid boundary particles are treated as described in Secs. III and IV, with the pairwise thermodynamic force applied only to fluid particle pairs. In order to prevent boundary penetration within the SDPD/hybrid domains, wall atoms are initialized on a lattice with a higher number density than the fluid ($\rho_n = 1.0$), and transition/SDPD fluid particles are specularly reflected at the solid-liquid interface, i.e., if a particle crosses the wall boundary, the velocity component of the particle normal to the wall is reversed such that it re-enters the fluid domain at the following time-step. The wall is translated in the x-direction with unit velocity. The thickness of the walls is 5 and the channel width is 13; in the x-direction, the SDPD and MD domains have a length of 8 and the buffers have a width of 5. Fluid atoms are initialized at the same number density and temperature as in the equilibrium study and with the same equation of state and corrective force magnitude for the buffer. The total number of particles is 6836. Due to the large number of hybrid particle interactions, this system setup

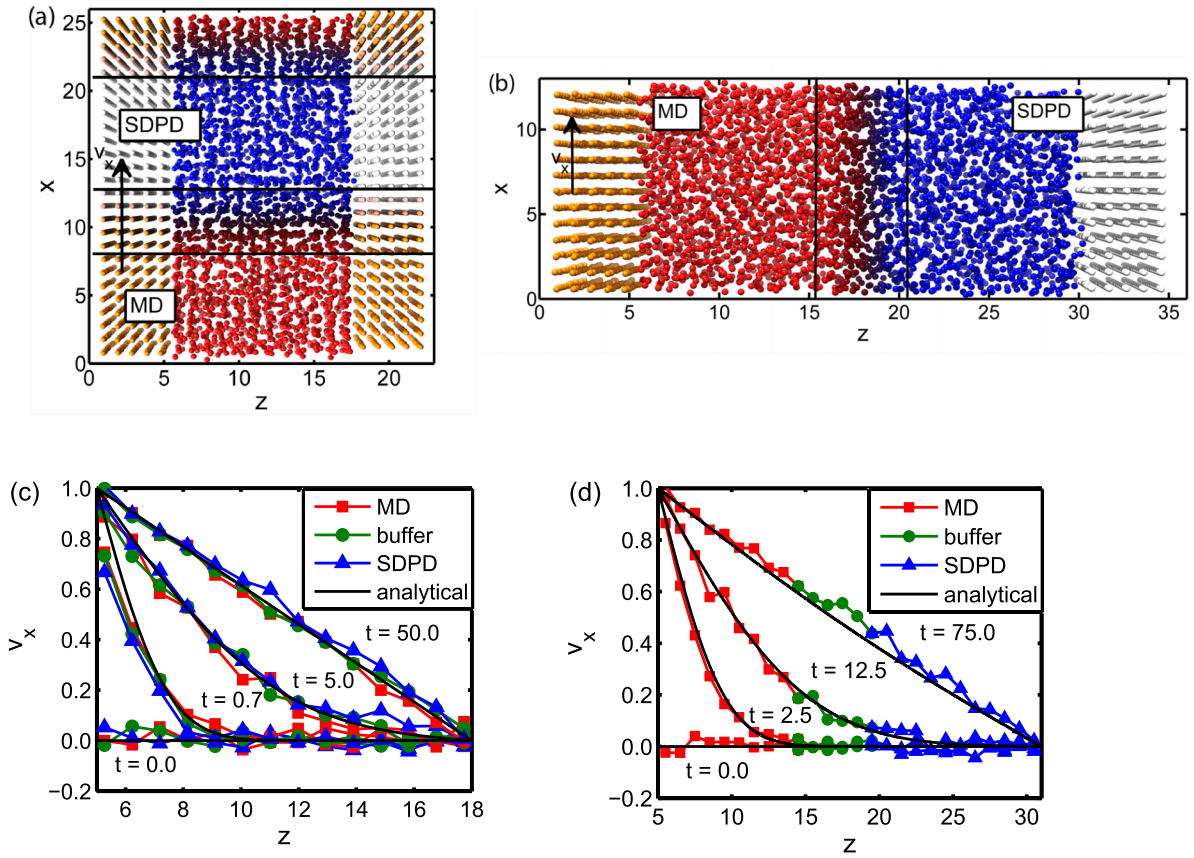

FIG. 4. Snapshots of the system for the (a) perpendicular and (b) parallel flow cases. (c) Velocity profiles for the MD, buffer, and SDPD domains for perpendicular start-up shear flow as compared to the analytical solution. (d) Velocity profiles for the parallel case. The velocities are averaged over 20 independent trajectories for both scenarios.

is not particularly efficient and is included to demonstrate the robustness of the technique with respect to the placement of the transition regions.

For the parallel case [Fig. 4(b)], the box dimensions are $13\times13\times36$ and the channel width is 26. The fluid atoms are initialized on a $12\times12\times24$ lattice between $z=5$ and 31, while wall atoms are initialized between $z=0$ and 5 and $z=31$ and 36 with number density $\rho_n=1.0$. This results in a total of 5146 particles. The buffer region boundaries are at $z=15.5$ and 20.5. In this case, one solid interface consists entirely of MD particles, while the other is always composed of SDPD particles; no transition between particle types ever occurs within each wall. Specular reflection is only required at the SDPD fluid-wall interface where the soft SDPD pressure force and high particle diffusivity can lead to boundary penetration. The MD harmonically tethered wall atoms are again held at a fixed temperature of $T=1$ using an Andersen thermostat and the equilibrium positions of the harmonic potential are translated with a velocity of 1. For both cases, we select $\Delta t=0.001$ and equilibrate for 5×10^4 steps before shearing.

Fig. 4(c) shows the velocity profiles for the perpendicular case in the MD, SDPD, and buffer regions at various times in the simulation. Rather than performing a local time average, results are averaged over 20 trajectories initialized with different random seeds in order to correctly capture hydrodynamics.[60,61] The MD fluid is thermostatted by both the harmonic oscillating walls in the atomistic region, as well as through contact with the fluid in the buffer. We find that the observed velocity profile in each region is in good agreement with the exact analytical solution. The absolute error in the velocity per bin, averaged over the simulation production trajectory and treating the analytical solution as exact, is approximately 0.021 in the buffer, 0.025 in the MD region, and 0.035 in the SDPD region. The average velocity in the channel approaches the expected linear profile at steady-state.

The velocity profiles for the parallel case are shown in Fig. 4(d), and are also in agreement with the exact continuum solution, with an averaged absolute error in the velocity profile of 0.025. At steady-state, there is a subtle deviation from the expected velocity profile in the buffer region between the MD and SDPD domains for the parallel case. This is due to the unphysical, spatially varying combination of forces, combined with the uniformly applied SDPD thermostat, which results in a fluid with a position-dependent viscosity. If better accuracy is required, this type of artifact in the dynamics may potentially be remedied by introducing a position-dependent thermostat as in Ref. 23. Since tuning the parameter p_0 may be used to improve the density distribution (Sec. V), we have also performed simulations for the parallel and perpendicular cases at a reduced absolute pressure of $p_0=0.8$ and find no appreciable difference in the results from the case with the true pressure.

VII. TRIPLE-SCALE SIMULATION OF SHEAR FLOW

One of the main motivations behind this multiscale approach is that it provides a natural interface between MD and continuum models. While the SDPD region considered in the examples in Secs. V and VI is of comparable molecular size, it is possible to further couple this domain to a series of continuum models of increasing length scale, all the way up to the non-fluctuating hydrodynamic limit. To illustrate how such a *hierarchy* of resolutions might work, we consider the parallel shear case and include one MD and two SDPD domains of different resolutions [Fig. 5(a)]. The strategy for bridging SDPD fluids with different smoothing lengths is described in Ref. 34 and thus we do not elaborate on that approach here. We choose a smoothing length for the coarse SDPD particles of $h=1.64$, which gives particles twice as massive as the finer SDPD ones next to the MD part of the system.

The triple-scale simulation is performed as follows. The global box dimensions are $13\times13\times57$. The MD wall has a thickness of 5 and atoms are again initialized at a higher density than the fluid ($13\times13\times5$ square lattice). Next to the wall, atomically resolved particles are initialized on a $12\times12\times24$ lattice across a volume with dimensions $13\times13\times26$, where particles within a distance of 10.5 to the wall are designated as MD atoms, particles between 10.5 and 15.5 units from the wall are hybrid particles, and beyond that particles are designated as a SDPD fluid with $h=1.3$. Adjacent to this domain is the coarse SDPD region, where particles are initialized on a square $9\times10\times19$ lattice over a region with volume $13\times13\times26$. Coarse particles within a distance of 6 from the box edge are designated as SDPD wall particles. The interface region between the fine and coarse SDPD domains has a width of 6 and is centered at the point initially separating these two regions. The coarse SDPD number density is half of that in the finely resolved region; hence, the number of particles in the simulation box is reduced by ~1746 as compared to the all-atom case to a total of 6011 particles. The equilibration time and time-step magnitude are the same as in Sec. VI.

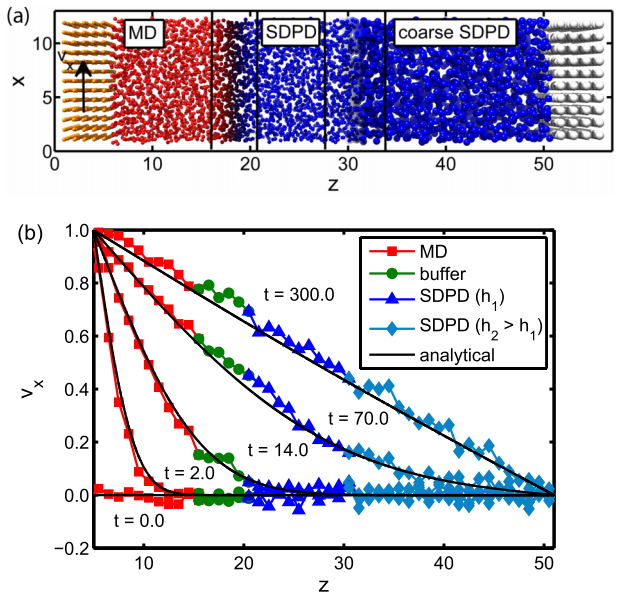

FIG. 5. (a) Visualization of the system for the parallel flow, triple-scale simulation. The coarse SDPD particles are twice as massive as the finely resolved ones, with half the number density. (b) Velocity profiles across the channel width for different times when the fluid is sheared. The exact solution is shown in black.

The system setup and time-dependent velocity profiles are illustrated in Fig. 5. Once again, we find that the transient solution, averaged over a set of 20 simulations, is in agreement with the analytical result throughout the entire problem domain. Hence, momentum is correctly transferred across the hierarchy of scales and regions of different resolutions such that dynamical flows are accurately reproduced.

VIII. CONCLUSION

In this paper, we describe a new hybrid MD-SDPD coupling strategy for interfacing a hierarchy of regions spanning a broad range of length scales from the molecular to the non-fluctuating continuum limit. This multiscale modeling approach has both advantages and limitations. In terms of advantages, the method ensures mass conservation in a very intuitive fashion and does not require iterative simulations to derive a new coarse-grained particle model if a different temperature or density becomes of interest, as would be the case for structure-, force-, or energy-matching approaches. Furthermore, there is no constraint on the atomistic model, provided that it is adequately described as a continuum fluid and the appropriate thermodynamic and transport properties at the desired temperature are known. However, as discussed in Secs. IV and V, the method does require knowledge of the system target density with corrections due to self-contribution effects, which necessitates running a short, pure SDPD simulation to calculate the overestimated densities at each particle as compared to the global system density.

In the multiscale approach, we couple MD to a region of SDPD particles with the same mass as those in the atomistic region. Since SDPD particles are interpreted as volumes of fluid, one obvious question is the validity of a SDPD fluid where the fluid volumes have the same size as the atoms in the MD region. The viability of a top-down, continuum approach at molecular scales is not immediately clear, particularly for non-homogeneous and complex fluids. In this respect, the atomically sized SDPD fluid might simply be interpreted as a convenient ansatz that successfully bridges continuum and MD worlds and that satisfies an appropriate number of constraints, including the fluctuation-dissipation theorem and basic conservation laws. Moreover, the continuum approximation often turns out to work surprisingly well when applied to molecular-scale problems (for instance, the accuracy of the Stokes-Einstein relation in predicting diffusivities), and this appears to be the case here. For the systems considered in this paper the approach is sufficient, although it may not be successful for more complicated fluids. Ultimately, this model provides a bridge between atomistic models and *increasingly* coarse SDPD regions. Through a hierarchy of SDPD domains with different resolutions, it is possible to coarse-grain to a scale where the SDPD model is appropriate.

Perhaps the most significant disadvantage of the presented MD-SDPD approach is that it does not decouple time scales. The maximum possible time-step is limited by the smallest characteristic time scale in the system, determined by the most finely resolved region in the domain. Even if the spatial domains are described by a range of length scales from molecular to highly coarse, all regions will be constrained to evolve over the same time scales. In this respect, the major computational savings would stem from a reduction in the number of particles describing the overall simulation, which of course can be quite significant in a simulation with a hierarchy of SDPD regions. However, an attractive feature of smoothed particle methods is that particle positions and velocity can be integrated in time using algorithms typically used in MD, and there exists a body of literature describing modified integrators that allow for multiple time-scales. Hence, it may be possible to use multiple time-scale integrators, such as ones originally developed for MD simulations by Tuckerman *et al.*,[62–67] to decouple time-scales between the coarse SDPD regions and finely resolved ones. In fact, the problem of decoupling time-scales in MD simulations containing particles with disparate masses has already been addressed,[62,63] although it is unclear if these techniques will work for SDPD.

In summary, this work demonstrates that it is possible to employ an adaptive resolution scheme in coupling a finely resolved, molecularly detailed part of a simulation domain treated via molecular dynamics to a fluctuating continuum domain. In contrast to earlier approaches that interface particle-based MD simulations with field-based finite-volume discretizations, the approach taken here involves representing the continuum solution using a particle-based technique, namely, smoothed dissipative particle dynamics. The overall strategy involves defining a buffer region in which particles smoothly change type when passing from the SDPD to MD domain and vice versa. Here, we have described how to design such a buffer in terms of specific interpolations of reversible interactions and the addition of "thermodynamic" forces that account for the change in particle types and minimize boundary artifacts. Such simple, modular, and hierarchical approaches in multiscale simulation are of growing importance in light of the wide range of problems that require the inclusion of multiple length scales. In this work, we consider a simple Lennard-Jones fluid and show that the MD-SDPD approach reproduces proper thermodynamic equilibrium globally, as well as accurate transient solutions to simple time-dependent hydrodynamic problems independent of the buffer region placement. Because of the success in previous studies using AdResS to couple MD fluids with more complicated molecular structure to spherically symmetric coarse-grained particles, we expect that this approach can be readily extended to coupling more complicated MD fluids to multiple SDPD domains.

ACKNOWLEDGMENTS

The authors gratefully acknowledge the support of the National Science Foundation (Award No. CBET-1256838) and a Dow Discovery Fellowship. Computational resources were provided by the Center for Scientific Computing from the CNSI, MRL: an NSF MRSEC (DMR-1121053) and NSF CNS-0960316. Molecular visualization was performed with the UCSF Chimera package. Chimera is developed by the Resource for Biocomputing, Visualization, and Informatics at the University of California, San Francisco (supported by NIGMS P41-GM103311).

[1]N. G. Hadjiconstantinou, J. Comput. Phys. **154**, 245 (1999).
[2]D. C. Tretheway and C. D. Meinhart, Phys. Fluids **16**, 1509 (2004).
[3]S. Thomas, A. Esmaeeli, and G. Tryggvason, Int. J. Multiphase Flow **36**, 71 (2010).
[4]C. L. Brooks III and M. Karplus, J. Chem. Phys. **79**, 6312 (1983).
[5]A. Brünger, C. L. Brooks III, and M. Karplus, Chem. Phys. Lett. **105**, 495 (1984).
[6]D. Beglov and B. Roux, Biopolymers **35**, 171 (1995).
[7]A. Okur, L. Wickstrom, M. Layten, R. Geney, K. Song, V. Hornak, and C. Simmerling, J. Chem. Theory Comput. **2**, 420 (2006).
[8]J. A. Wagoner and V. S. Pande, J. Chem. Phys. **134**, 214103 (2011).
[9]S. T. O'Connell and P. A. Thompson, Phys. Rev. E **52**, R5792 (1995).
[10]N. G. Hadjiconstantinou and A. T. Patera, Int. J. Mod. Phys. C **08**, 967 (1997).
[11]X. B. Nie, S. Y. Chen, W. N. E, and M. O. Robbins, J. Fluid Mech. **500**, 55 (2004).
[12]R. Delgado-Buscalioni and G. De Fabritiis, Phys. Rev. E **76**, 036709 (2007).
[13]R. Delgado-Buscalioni and P. V. Coveney, Phys. Rev. E **67**, 046704 (2003).
[14]R. Delgado-Buscalioni, E. G. Flekkøy, and P. V. Coveney, Europhys. Lett. **69**, 959 (2005).
[15]R. Delgado-Buscalioni, P. V. Coveney, G. D. Riley, and R. W. Ford, Philos. Trans. R. Soc., A **363**, 1975 (2005).
[16]L. D. Landau and E. M. Lifshitz, *Fluid Mechanics*, 2nd ed. (Butterworth-Heinemann, Amsterdam, 1987), Vol. 6.
[17]N. Hadjiconstantinou, Bull. Pol. Acad. Tech. Sci. **53**, 335 (2005).
[18]D. A. Fedosov and G. E. Karniadakis, J. Comput. Phys. **228**, 1157 (2009).
[19]A. Dupuis, E. M. Kotsalis, and P. Koumoutsakos, Phys. Rev. E **75**, 046704 (2007).
[20]M. Praprotnik, L. Delle Site, and K. Kremer, J. Chem. Phys. **123**, 224106 (2005).
[21]M. Praprotnik, L. Delle Site, and K. Kremer, Phys. Rev. E **73**, 066701 (2006).
[22]M. Praprotnik, S. Matysiak, L. D. Site, K. Kremer, and C. Clementi, J. Phys.: Condens. Matter **19**, 292201 (2007).
[23]S. Matysiak, C. Clementi, M. Praprotnik, K. Kremer, and L. Delle Site, J. Chem. Phys. **128**, 024503 (2008).
[24]R. Delgado-Buscalioni, K. Kremer, and M. Praprotnik, J. Chem. Phys. **131**, 244107 (2009).
[25]S. Poblete, M. Praprotnik, K. Kremer, and L. D. Site, J. Chem. Phys. **132**, 114101 (2010).
[26]S. Fritsch, S. Poblete, C. Junghans, G. Ciccotti, L. Delle Site, and K. Kremer, Phys. Rev. Lett. **108**, 170602 (2012).
[27]R. Potestio, S. Fritsch, P. Español, R. Delgado-Buscalioni, K. Kremer, R. Everaers, and D. Donadio, Phys. Rev. Lett. **110**, 108301 (2013).
[28]L. B. Lucy, Astron. J. **82**, 1013 (1977).
[29]R. A. Gingold and J. J. Monaghan, Mon. Not. R. Astron. Soc. **181**, 375 (1977).
[30]G. R. Liu and M. B. Liu, *Smoothed Particle Hydrodynamics: A Meshfree Particle Method* (World Scientific Publishing Company, 2003).
[31]P. Español and M. Revenga, Phys. Rev. E: Stat., Nonlinear, Soft Matter Phys. **67**, 026705 (2003).
[32]W. Dzwinel, W. Alda, and D. A. Yuen, Mol. Simul. **22**, 397 (1999).
[33]G. C. Ganzenmüller, S. Hiermaier, and M. O. Steinhauser, Eur. Phys. J.: Spec. Top. **206**, 51 (2012).
[34]P. M. Kulkarni, C.-C. Fu, M. S. Shell, and L. Gary Leal, J. Chem. Phys. **138**, 234105 (2013).
[35]A. Vázquez-Quesada, M. Ellero, and P. Español, J. Chem. Phys. **130**, 034901 (2009).
[36]S. Litvinov, M. Ellero, X. Hu, and N. A. Adams, Phys. Rev. E **77**, 066703 (2008).
[37]S. Litvinov, X. Y. Hu, and N. A. Adams, J. Phys.: Condens. Matter **23**, 184118 (2011).
[38]N. Moreno, P. Vignal, J. Li, and V. M. Calo, Procedia Comput. Sci. **18**, 2565 (2013).
[39]X. Bian, S. Litvinov, R. Qian, M. Ellero, and N. A. Adams, Phys. Fluids **24**, 012002 (2012).
[40]A. Vázquez-Quesada, M. Ellero, and P. Español, Phys. Rev. E **79**, 056707 (2009).
[41]S. R. D. Groot and P. Mazur, *Non-Equilibrium Thermodynamics*, Dover ed. (Dover Publications, New York, 2011).
[42]M. Grmela and H. C. Öttinger, Phys. Rev. E **56**, 6620 (1997).
[43]H. C. Öttinger and M. Grmela, Phys. Rev. E **56**, 6633 (1997).
[44]H. C. Oͤttinger, *Beyond Equilibrium Thermodynamics* (Wiley-Interscience, Hoboken, NJ, 2005).
[45]P. Español, Phys. Rev. E **57**, 2930 (1998).
[46]J. J. Monaghan and J. C. Lattanzio, Astron. Astrophys. **149**, 135 (1985).
[47]J. J. Monaghan, Comput. Phys. Rep. **3**, 71 (1985).
[48]A. P. Whitworth, A. S. Bhattal, J. A. Turner, and S. J. Watkins, Astron. Astrophys. **301**, 929 (1995).
[49]O. Flebbe, S. Munzel, H. Herold, H. Riffert, and H. Ruder, Astrophys. J. **431**, 754 (1994).
[50]J. P. Morris, P. J. Fox, and Y. Zhu, J. Comput. Phys. **136**, 214 (1997).
[51]See supplementary material at http://dx.doi.org/10.1063/1.4905720 for a detailed description of the multiscale approach and discussion of Morris boundary conditions for enforcing no-slip in smoothed dissipative particle dynamics simulations.
[52]J. J. Monaghan, J. Comput. Phys. **82**, 1 (1989).
[53]D. M. Heyes, J. Chem. Phys. **132**, 064504 (2010).
[54]T. C. Beutler, A. E. Mark, R. C. van Schaik, P. R. Gerber, and W. F. van Gunsteren, Chem. Phys. Lett. **222**, 529 (1994).
[55]R. D. Groot and P. B. Warren, J. Chem. Phys. **107**, 4423 (1997).
[56]T. Soddemann, B. Dünweg, and K. Kremer, Phys. Rev. E **68**, 046702 (2003).
[57]K. Meier, A. Laesecke, and S. Kabelac, J. Chem. Phys. **122**, 014513 (2004).
[58]R. L. Rowley and M. M. Painter, Int. J. Thermophys. **18**, 1109 (1997).
[59]K. Meier, A. Laesecke, and S. Kabelac, J. Chem. Phys. **121**, 3671 (2004).
[60]S. Orlandini, S. Meloni, and G. Ciccotti, Phys. Chem. Chem. Phys. **13**, 13177 (2011).
[61]S. Orlandini, S. Meloni, and G. Ciccotti, AIP Conf. Proc. **1332**, 77–95 (2011).
[62]M. Tuckerman, B. J. Berne, and G. J. Martyna, J. Chem. Phys. **97**, 1990 (1992).
[63]M. E. Tuckerman, B. J. Berne, and A. Rossi, J. Chem. Phys. **94**, 1465 (1991).
[64]M. E. Tuckerman and B. J. Berne, J. Chem. Phys. **95**, 8362 (1991).
[65]M. E. Tuckerman, B. J. Berne, and G. J. Martyna, J. Chem. Phys. **94**, 6811 (1991).
[66]M. E. Tuckerman, B. J. Berne, and A. Rossi, J. Chem. Phys. **94**, 1465 (1991).
[67]M. E. Tuckerman, G. J. Martyna, and B. J. Berne, J. Chem. Phys. **93**, 1287 (1990).
[68]We use W in reference to both the Wiener process and the smoothing function for historical reasons, though the two are unrelated.